Research Square

Preprints are preliminary reports that have not undergone peer review.
They should not be considered conclusive, used to inform clinical practice,
or referenced by the media as validated information.

Repeated xylitol production by immobilized Gluconobacter oxydans using diatom frustule–alginate composite carriers

Dong Liu

liudong2021@ytu.edu.cn

Yantai University

Jin-Cheng Guo

Yantai University

Jun-Hao Su

Yantai University

Lu Liu

Yantai University

Shuo-Nan Cao

Yantai University

Bo-Hou Yang

Yantai University

Hai-Ling Zhang

Yantai University

Research Article

Keywords: Xylitol, Gluconobacter oxydans, Immobilization, Diatom frustule, Sodium alginate

Posted Date: July 2nd, 2026

DOI: https://doi.org/10.21203/rs.3.rs-10081907/v1

License: This work is licensed under a Creative Commons Attribution 4.0 International License.
Read Full License

Additional Declarations: No competing interests reported.

Abstract

Xylitol, a common sugar substitute in food and pharmaceuticals, can be produced microbially using glucose as the primary substrate. Our earlier study established an efficient one-step biotransformation system in *Gluconobacter oxydans* that converts D-arabitol to xylitol. To improve the reusability of resting cells, recombinant *G. oxydans* was immobilized in a composite matrix of *Cyclotella meneghiniana* frustules and solium alginate. The combined approach not only enhanced the mechanical strength and stability of the beads but also facilitated mass and oxygen transfer. Compared with frustules adsorption and alginate encapsulation alone, the combined immobilized cells exhibited increases in catalytic activity of 32.8% and 17.3%, respectively. An in-situ immobilization protocol, adding 2.0 g/L frustules to the fermentation medium with a 22 h culture time, further improved immobilized cell activity by 17.3%. Moreover, frustule-adsorbed cells cross-linked with 0.5% glutaraldehyde (GA) exhibited enhanced catalytic performance in continuous batch operation. Finally, the repeated biotransformation was carried out by immobilized *G. oxydans*, achieving an average xylitol titer of 15.44 g/L over six consecutive cycles. This study presents a practical immobilization strategy for xylitol production and offers a reference for microbial production of other biochemicals.

1. Introduction

Xylitol, a five-carbon sugar alcohol, is widely used as a low-calorie sweetener and humectant in the food and pharmaceutical industries [1]. A biotechnological route using glucose as the substrate is an efficient method for xylitol production [2]. The process involves three steps: glucose is first converted to D-arabitol by osmophilic yeasts; the membrane-bound D-arabitol dehydrogenase (mAraDH) of *Gluconobacter oxydans* then converts D-arabitol to D-xylulose; finally, the soluble xylitol dehydrogenase (XDH) in *G. oxydans* reduces D-xylulose to xylitol [2]. In this pathway, the catalytic activity of XDH and limited NADH availability are key bottlenecks [3]. In our previous study, through molecular modification of XDH combined with cofactor engineering, an efficient xylitol synthesis system was established in *G. oxydans*.

G. oxydans is an obligate aerobic bacterium known for selectively converting sugars into value-added alcohols and sugar derivatives [4]. However, free-cell systems for xylitol production suffer from limited reusability, operational instability, and difficulty cell washout. It has been reported that harsh production condition of high acidity, elevated osmolarity, and agitation caused a sharp decline in *G. oxydans* catalytic activity after only three consecutive batches [5]. Immobilized cell systems have therefore been considered to improve process productivity and reduce production costs, offering advantages over free-cell fermentation in stability and recyclability. To date, *G. oxydans* has been immobilized on carriers including corncob, porous ceramics, and diatomite, and recent advances include 3D-printed scaffolds and nanocellulose [6–10]. In this study, we aim to screen and identify suitable immobilization materials to improve the batch production efficiency of recombinant *G. oxydans*.

Nanostructured biomaterials have recently attracted attention as promising alternatives to synthetic nanomaterials due to their scalability, low environmental impact, high structural reproducibility, and low production costs [11]. Conventional inorganic silica materials, such as silica and diatomite (DE), are widely used for whole-cell and enzyme immobilization but present several challenges [12]. For example, DE is derive from fossilized diatom remains and occurs as blocks or aggregates with variable size and shape because of the mixture of multiple diatom species [12, 13]. In contrast, diatom frustules, the bio-silica shells of single-celled photosynthetic diatoms, exhibit ordered, species-specific pore patterns and hierarchical pore organization. As a result of their high abundance, compositional purity, and structural uniformity, these frustules possess superior mechanical strength and toughness compared to bulk silica or diatomite, making them ideal candidates for cell adsorption and immobilization [14, 15]. As a typical central diatom, *Cyclotella meneghiniana* has a disc-shaped morphology with marginal fultoportulae and nano-pores on the disc surface, which confer high specific surface area and excellent oxygen diffusion for cell adsorption[16, 17] (Fig. 1). Therefore, the diatom frustules of *C. meneghiniana* were selected as the adsorption carrier for immobilizing the recombinant *G. oxydans*.

Cell immobilization on solid carriers typically occurs via physical adsorption-hydrogen bonds, van der Waals forces, and hydrophobic interactions between the cell membrane and the support. These weak forces can lead to cell detachment during prolonged or continuous batch catalysis. An alternative widely used approach is cell entrapment, in which cells are confined within gel matrices such as natural polymers (e.g., alginate, carrageenan) or synthetic polymers (e.g., polyvinyl alcohol, polyacrylamide) [10]. Alginate is frequently employed as an immobilization carrier because of its low cost, ease of handling, good biocompatibility, and resistance to microbial degradation. However, sodium alginate gels suffer from limited mechanical strength and poor mass transfer. To enhance internal oxygen diffusion, previous studies co-immobilized oxygen carriers such as n-dodecane, silicone oil, perfluorodecalin, and hemoglobin with cells in alginate beads; however, these additives can alter cell physiology and complicate downstream processing [18, 19]. Incorporating diatom frustules can modify the structural design of alginate-immobilized cells due to its nano-porous and fultoportulae structure, thereby extending the operational lifetime of the immobilized system. So far, leveraging the complementary advantages of organic and inorganic supports, many studies have adopted composite carriers for biocatalysis. For example, Cheng eta al. immobilized *Burkholderia vietnamiensis* C09V on PVA-alginate-kaolin gel beads, which enhanced the degradation of crystal violet from aqueous solution [17]. For *G. oxydans*, the combined immobilization of porous diatom frustules and sodium alginate was selected as a potential method for xylitol production.

The objective of this study was to investigate the effects of using a novel combination immobilization carrier material on the conversion of D-arabitol to xylitol in the recombinant *G. oxydans*. Naturally porous frustules from *C. meneghiniana* were incorporated into sodium-alginate beads to improve oxygen diffusion and mechanical integrity. We assessed these frustules as a low-cost biomaterial for cell immobilization, examining effects on catalytic activity, operational stability, and reusability, with the goal of establishing an efficient continuous process for xylitol production.

2. Materials and method

2.1 Strains, plasmids, media, and culture conditions

G. oxydans/XDH-GDH used in this study was stored at 4°C on a SY agar slant, and transferred monthly. The seed medium was composed of 55.0 g sorbitol, 25.0 g yeast extract, 5.0 g K_2HPO_4, and 5.0 g KH_2PO_4 per liter, pH 6.0. The fermentation medium was composed of 80.0 g sorbitol, 25.0 g yeast extract, 5.0 g K_2HPO_4, and 5.0 g KH_2PO_4, pH 6.0. All media were autoclaved for 20 min at 121°C. For seed preparation, the liquid seed was prepared by transferring cells from a 36-h-old agar slant into 250 mL flasks, which contained 50 mL of liquid seed medium, and the flasks were incubated on a rotary shaker at 150 rpm for 48 h at 30°C. Liquid seed medium (0.5 mL) was inoculated into a 500 mL Erlenmeyer flask containing 100 mL fermentation medium. The flasks were incubated in an orbital shaker (150 rpm, 30°C) for 24 h.

2.2 Genetic operations

The enhanced green fluorescent protein (eGFP) gene was amplified by PCR from pET28a-eGFP using primers listed in Table 1. The amplified fragment was cloned into the *N*-terminus of *xdh* in pBBR-*gHp0169-xdh*$_{M3}$*-gdh-vhb* using ClonExpress®II One Step Cloning Kit to generate the fusion plasmid pBBR-*gHp0169-xdh*$_{M3}$*-gdh-vhb*. Plasmid was then introduced into *G. oxydans* by triparental mating and selected on gentamicin, yielding recombinant strains *G. oxydans*/XDH$_{M3}$-eGFP-GDH-VHb.

Table 1
Primers used in this study

Primer	Sequence (5'-3')
eGFP-F	CATTGTTGCCATGTATCAAatggtgagcaagggcgagg
eGFP-R	gacagtcaccgagtacactTTActtgtacagctcgtcc
pBBR-*gHp0169-xdh-gdh-vhb*-F	TAAAGTGTACTCGGTGACTGTCGATCCGGCTGCTAAC
pBBR-*gHp0169-xdh-gdh-vhb*-R	TTGATACATGGCAACAATGG

2.3 Activity assay of *G. oxydans*

The activity of *G. oxydans* was determined by measuring the initial formation rate of D-xylulose within the 6 h performed in a basal reaction mixture consisted of 15 g/L D-arabitol, and an appropriate number of resting cells collected from 100 mL fermentation broth. The concentration of D-xylulose was determined using high-performance liquid chromatography (HPLC). One unit of *G. oxydans* activity (U) towards D-arabitol was defined as the amount of *G. oxydans* that catalyzes the formation of 1 μmol D-xylulose per min.

2.4 Preparation of diatom frustules

Cultivated algal biomass (algal sludge) was freeze-dried for 20 h to obtain algal powder. A total of 0.5 g of algal powder was mixed with 30 mL of 90% methanol to remove organic matter. The mixture was ultrasonically disrupted in an ice bath (600 W, 2 s/4 s), then treated in a boiling water bath for 10 min and centrifuged at 9000×g for 10 min to collect the precipitate. The washing step was repeated twice. The precipitate was resuspended in 10% (v/v) HCl and gently stirred at 200 rpm for 2 h at 60°C to remove residual organic matter. After cooling to room temperature, the mixture was filtered under vacuum and washed repeatedly with deionized water until the pH of the filtrate reached approximately 7.0. The precipitate was then freeze-dried.

Decolorization of diatom frustules was carried out by oxidative treatment using $K_2Cr_2O_7$. First, 1.0 g of diatom frustules was placed in a digestion flask and mixed with 300 mL deionized water and 50 mL potassium dichromate solution (20 mM). The flask was then placed on a digestion block, and 10 mL of concentrated H_2SO_4 was added. The mixture was digested for 2 h, followed by vacuum filtration and repeated washing with deionized water until the filtrate pH was approximately 7.0. The resulting precipitate was then freeze-dried to obtain purified diatom frustules.

2.5 Optimization of immobilization conditions

Adsorption of *G. oxydans* on diatom frustules

To adsorb *G. oxydans* on diatom frustules, the cell pellet was collected by centrifugation from 100 mL of fermentation broth prepared according to Section 2.1. Treated diatom frustules (0.2 g) were mixed with the resting cells in 5 mL of deionized water, and the suspension was stirred at 150 rpm on a magnetic stirrer for 3 h at room temperature. After adsorption, the frustule-adsorbed cells were separated by vacuum filtration.

Preparation of calcium alginate beads

Calcium alginate beads were prepared by thoroughly mixing resting cells with 2.0% (w/v) sodium alginate solution and pumping the mixture through a peristaltic pump into 2.0% (w/v) $CaCl_2$. The formed beads were packed uniformly and stored in $CaCl_2$ solution at 4°C for 3 h, and washed with deionized water to remove residual $CaCl_2$ prior to use.

Combined adsorption-entrapment immobilization

For combined immobilization, the frustule-adsorbed cells were mixed with 2.0% (w/v) sodium alginate solution, and the mixture was then passed through a peristaltic pump into a 2.0% (w/v) $CaCl_2$ solution. After washing, the co-immobilized *G. oxydans* were obtained.

In-situ adsorption during fermentation

For in-situ adsorption, pretreated diatom frustules were added to the fermentation medium at concentrations of 0.5, 1.0, 1.5, 2.0, 2.5, and 3.0 g/L. After inoculation, the culture was incubated at 30°C,

180 rpm for 24 h. At the end of fermentation, the frustules-adsorbed cells were collected by centrifugation at 9000×g for 10 min, and subsequent entrapment was performed as described above.

Optimization of sodium alginate and $CaCl_2$ concentrations

The optimal concentration of sodium alginate and $CaCl_2$ were measured. The sodium alginate concentrations tested are 1.0, 1.5, 2.0, 2.5 and 3.0% (w/v). Embed the crosslinked cells in sodium alginate and use an electronic peristaltic pump to drop the cell suspension into $CaCl_2$ solutions at final concentrations of 1.0, 2.0, 3.0, 4.0 and 5.0% (w/v).

Activity assay

The supernatant was analyzed by HPLC to determine D-xylulose concentration, and the activity assay for immobilized *G. oxydans* was performed as described in Section 2.3.

2.6 Cross-linking agent screening experiment

Several crosslinkers were evaluated to immobilize *G. oxydans* onto diatom frustules: the bifunctional aldehyde glutaraldehyde (GA), the epoxy crosslinker poly (ethylene glycol) diglycidyl ether (PEGDGE), neopentyl glycol diglycidyl ether (NGDE), and dopamine hydrochloride (DA). Each crosslinker (0.5% w/v) was added to a suspension of the diatom frustules-adsorbed *G. oxydans* in water and stirred at room temperature for 1 h. The mixture was centrifuged at 9000×g for 10 min, and the precipitate was washed repeatedly with deionized water until the pH of the filtrate reached approximately 7.0. Then the crosslinked cells encapsulated in 2.0% sodium alginate solution with 2.0% $CaCl_2$. To evaluate crosslinking efficiency, immobilized cells were applied in six consecutive catalytic runs; each batch contained 15 g/L D-arabitol and was conducted at 30°C and 180 rpm for 12 h. The supernatant from each batch was analyzed by HPLC to quantify D-xylulose, and the activity assay for immobilized *G. oxydans* was performed as described in Section 2.3.

2.7 Cell cultivation in a stirred bioreactor

The cell cultivation process was carried out in a 5-L multi-bioreactor system (BLBIO-50SJ-5, China) using fermentation medium. A 10% (v/v) inoculum was added to a stirred bioreactor containing medium with 2 g/L diatom frustules and incubated at 30°C with stirring at 600 rpm and aeration of 1.5 vvm for 24 h. The cultivation broth (600 mL) was centrifuged at 9000×g for 10 min. The frustules-adsorbed cells were crosslinked with 0.5% glutaraldehyde (GA) and then embedded in 2.0% (w/v) sodium alginate solution to obtain the final immobilized cells.

2.8 Reusability of immobilized *G. oxydans*

The reusability of immobilized *G. oxydans* was evaluated over six consecutive cycles. Each cycle was carried out by incubating immobilized *G. oxydans* in 50 mL water containing 30 g/L D-arabitol with 20 g/L $CaCO_3$ to maintain pH. Reactions were performed at 35°C and 180 rpm for 40 h. And 20 g/L glucose was

added at 10 h to facilitate NADH regeneration. After each run, immobilized *G. oxydans* was recovered and washed with water to remove residual substrate, then transferred to fresh reaction solution, and the supernatant was collected for xylitol quantification by HPLC.

2.9 Analytical methods

2.9.1 Determination of cell biomass

Biomass concentration in samples was determined by measurement of optical density at 600 nm. The values of optical density were transformed to dry cell weight (DCW) through calibration dependence. The standard curve between the DCW and OD_{600} was y = 0.4627x-0.2685, R^2 > 0.99. All experiments were performed in triplicate, and the mean values and standard curves calculated from three different batches of data were used in the manuscript.

2.9.2 Fluorescence microscopy

Expression of recombinant cells containing eGFP-fused proteins was observed with confocal fluorescence microscopy using a Leica TCS SP8 microscope (Leica, Wetzlar, Germany). The mutant cells grown in liquid medium were collected at the logarithmic growth phase. Chlorophyll autofluorescence was evaluated from the emission between 600 and 750 nm by excitation with a 552-nm laser. EGFP was excited by a 488-nm laser, and green fluorescence was detected at 500 to 520 nm.

2.9.3 Determination of xylose and D-xylulose

The HPLC was used to accurately measure the quantities of substrates and products. The concentration of D-arabitol, D-xylulose, and xylitol was assayed by HPLC with a differential refractive index detector (Waters, USA), with an Aminex HPX-87H column (300 mm×7.8 mm; Bio-Rad, Hercules, CA) at 55 ^{o}C with a flow rate of 0.5 mL/min and 5 mM H_2SO_4 as the eluent.

3. Results and discussion

3.1 Immobilization condition optimization

In a previous study, we developed a whole-cell catalytic process for producing xylitol from D-arabitol using engineered *G. oxydans* through molecular modification and cofactor engineering. In this study, to improve reusability and lower costs, the recombinant cells were immobilized by adsorption onto diatom frustules. Frustules of *C. meneghiniana*, characterized by a hierarchically nano-porous architecture and rough surfaces, were selected as an adsorption matrix. Frustules were isolated using an optimized protocol, sequentially treated with methanol and hydrochloric acid to obtain purified frustules as adsorption matrix for cell immobilization. Compared with free cells, immobilization on frustules reduced apparent enzyme activity by 41.6% (Fig. 2). This reduction attributed to the limited cell-binding capacity of the frustules, resulting in substantial cell loss during immobilization.

In a separate set of experiments, recombinant cells were immobilized by entrapment within a porous matrix of sodium alginate. Although cells immobilized solely in sodium alginate retained most of the initial activity (66.1%) than frustules adsorption alone, oxygen diffusion within the dense gel remained restricted. To address the limitations of both single-matrix systems, cells pre-adsorbed on frustules were encapsulated in sodium alginate beads, which not only retain the cells but protect them from environmental stressors. This combined immobilization strategy (alginate + frustules) increased the activity of *G. oxydans* by 32.8% and 17.3% compared with frustules adsorption and alginate encapsulation alone (Fig. 2). The diatom frustules embedded in the beads exhibited a porous architecture that permitted substrate and oxygen diffusion into the internal pores while maintaining high mechanical strength. In addition, continuous consumption of D-arabitol by encapsulated cells generated an inward-directed substrate concentration gradient that mitigated substrate inhibition.

3.2 In-situ immobilization of *G. oxydans* by diatom frustules

Previous studies developed an in-situ adsorption approach by adding immobilization carriers, such as porous glass, sugarcane bagasse, or nanocellulose, directly to the fermentation medium [20, 21]. During attachment to the immobilization matrix, cells secrete a mucilaginous glycocalyx that promotes agglomeration on the solid support and facilitates adhesion [22]. Immobilizing cells during growth offers several benefits, including high adsorption efficiency, increased specific growth rates, and reduced processing time [23]. Consequently, in-situ immobilization has attracted considerable attention and has been widely applied in repeated-batch fermentations for the production of ethanol, human lysozyme, amino acids, and other bioproducts.

In this study, cells were immobilized in-situ by natural adsorption through direct contact with diatom frustules during biomass proliferation. Different amounts of diatom frustules were added to the growth medium, and the adsorbed cells were subsequently entrapped in sodium alginate. As shown in Fig. 3a, the volumetric activity of immobilized cells rose with increasing frustule concentration before declining at higher loadings. The highest enzyme activity (7.06 U/L) were observed at frustules loading of 2.0 g/L, representing a 17.3% increase compared with the post-culture adsorption method. This enhancement likely reflects the biocompatibility of the frustule surface, which, together with the exopolysaccharides, promoted cell adhesion to hydrophobic surfaces. A previous report indicated that the in-situ adsorption process reaches a dynamic equilibrium between adsorbed and freely suspended cells, causing cell detachment and relocation [22]. To achieve the optimal in-situ adsorption immobilization, cultivation time was evaluated. As shown in Fig. 3b, the enzymatic activity of immobilized cells increased with fermentation time, reached maximum values of 7.12 U/L at 22 h. The study found no decrease in enzyme activity, indicating that cell adsorption onto the diatom frustules increased as biomass grew. Therefore, the optimal immobilization performance was achieved by adding 2.0 g/L diatom frustules during growth for 22 h, followed by encapsulation in sodium alginate. Overall, this in-situ adsorption approach enhanced frustule binding efficiency and produced immobilized whole-cell biocatalysts that exhibited improved performance in reactions.

The concentration of $CaCl_2$, sodium alginate, and bead size were further optimized. As shown in Fig. 4a, increasing the $CaCl_2$ concentration up to 3.0% (w/v) resulted in a progressive increase in immobilized enzyme activity to 7.46 U/L, with no further gain at higher concentrations. However, sodium alginate concentration had no significant effect on immobilized cell activity (Fig. 4b), likely because these concentrations of gel can provide sufficient mechanical strength and an adequate pore network to support oxygen supply and mass transfer for *G. oxydans*. In contract, alginate concentration markedly affected bead morphology and physical state (Fig. 5). At 1.0% no intact beads formed due to low viscosity; at 1.5-2.0% well-shaped, uniform beads were produced, with 2.0% giving the best molding; above 2.5% excessive viscosity led to irregular, deformable beads. Thus, 2.0% sodium alginate was selected for immobilization. Regarding bead size, the highest enzyme activity was obtained with 3.0-mm beads, likely due to the higher surface-to-volume ratio associated with smaller bead diameters, which facilitated mass transfer. The strategy of combining diatom frustules with sodium alginate for whole-cell immobilization provides an effective approach for xylitol production.

3.3 Effect of crosslinkers on the immobilization of frustules

Addition of crosslinking agents enables covalent bond formation between cells and the immobilization matrix, resulting in robust fixation onto the carrier surface. To enhance attachment and stability of *G. oxydans* immobilized on diatom frustules the in-situ frustules-adsorbed cells were treated with GA, PEGDGE, NGDE and DA. The crosslinked cells were subsequently entrapped in sodium alginate beads for six consecutive catalytic runs. As shown in Fig. 6, crosslinked cells exhibited lower relative activity than non-crosslinked controls in the first batch, likely because covalent cross-linking damaged cell membrane integrity. However, with increasing number of catalytic batches, the enzymatic activity of crosslinked cells gradually surpassed that of the non-crosslinked samples. After six runs, GA-crosslinked preparations retained 64.6% of initial activity, compared with 53.3% for PEGDGE, 54.6% for NGDE, 50.4% for DA and 41.7% for non-crosslinked samples. GA-crosslinked preparations exhibited the highest immobilized-cell activity and the greatest operational stability, whereas PEGDGE, NGDE, and DA treatments showed lower enzyme retention and faster activity loss. The superior performance of GA reflects its ability to cross-link cell-surface amines, forming Schiff-base linkages that reinforce cell-carrier interactions and produce insoluble aggregates [15]. These results indicated that optimized GA crosslinking is an effective strategy for improving the performance of diatom frustule-based whole-cell immobilization.

3.4 Characterization of immobilized enzyme

Fluorescence staining showed a single dense fluorescent mass on the frustule surface, dominated by green signal and lacking distinct colony morphology. It indicated that *G. oxydans* forms compact, viable aggregates concentrated on the frustule surface rather than discrete colonies (Fig. 7).

3.5 Reusability and storage stability of immobilized *G. oxydans*

Repeated use is a major advantage of immobilized cells because it reduces cell loss, saves time, and lowers cultivation costs. Accordingly, the prepared biocatalyst was tested in six batch reactions converting D-arabitol to xylitol. As shown in Fig. 8, the initial batch yielded 17.79 g/L xylitol from 30 g/L D-arabitol within 40 h. Xylitol production declined in subsequent batches, but the decrease was slower for the immobilized system, yielding an average of 15.44 g/L after six consecutive cycles. Entrapment in alginate beads provides a protective matrix that shields *G. oxydans* from environmental stress, while the porous diatom frustules embedded in the beads facilitate substrate and oxygen diffusion into the interior; their synergy enables efficient biocatalysis. Notably, the sodium alginate beads remained intact with no detectable cell leakage even after ten consecutive batches, demonstrating superior structural integrity and operational stability compared with previous reports. This enhanced durability is attributed to immobilized cells lodged within diatom frustules inside the beads, which stabilize the microbial system and sustain high D-arabitol catalytic activity. Furthermore, the insolubility of sodium alginate simplifies cell washout, eliminating the need for time-consuming centrifugation to harvest the reaction supernatant. Collectively, these results confirm that sodium alginate combined with diatom frustules provides a protective, stable microenvironment that mitigates inhibition and improves the operational stability of microbial cells.

Beads composed of sodium alginate and diatom frustules were stored at 4°C to assess immobilized cell stability. After over two months, enzymatic activity remained above 90%, demonstrating excellent retention of function. The frustule–gel matrix likely shields cells from drying, physical damage, and inhibitory agents during cold storage. Thus, the immobilized system supports prolonged storage and ready reuse, easing operational demands and lowering the need for frequent culture renewal.

4. Conclusion

In this study, recombinant *G. oxydans* successfully immobilized using a combined strategy of adsorption onto diatom frustules and entrapment in sodium alginate for the bioconversion of D-arabitol to xylitol. The alginate beads preserved cell integrity, while the frustules' natural porous architecture enhanced mass and oxygen transfer within the beads. We also developed an effective in-situ adsorption immobilization method using diatom frustules with a 22-h culture time showed the maximizing performance. Moreover, frustules crosslinked with 0.5% GA retained high activity in continuous biocatalysis. The immobilized cells maintained high activity over six cycles, yielding an average xylitol titer of 15.44 g/L. Collectively, these results demonstrate that the combination of diatom frustules and sodium alginate provides an effective and robust immobilization strategy for the consecutive conversion of D-arabitol to xylitol.

Declarations

Ethics approval and consent to participate

Not applicable.

Consent for publication

Not applicable.

Availability of data and materials

The datasets used and/or analyzed during the current study are available from the corresponding author on reasonable request.

Competing Interests

The authors declare no competing interests.

Funding

This work was financially supported by the Natural Science Foundation of Shandong Province (Grant number: ZR2022QB111).

CRediT authorship contribution statement

DL performed the conceptualization, methodology, data curation, writing-original draft and writing-review & editing. JG performed the investigation and validation, data curation, writing-original draft and writing-review & editing. JS, LL, SC, and BY performed the formal analysis, methodology, and writing review & editing. HZ performed the conceptualization, supervision and project administration.

Acknowledgements

Not applicable.

References

1. Rao LV, Goli JK, Gentela J, Koti S (2016) Bioconversion of lignocellulosic biomass to xylitol: an overview. Bioresour Technol 213:299–310
2. Diptarka Dasgupta DD, Sheetal Bandhu SB, Adhikari DK, Debashish Ghosh DG (2017) Challenges and prospects of xylitol production with whole cell bio-catalysis: a review
3. Suzuki Si, Sugiyama M, Mihara Y, Hashiguchi Ki, Yokozeki K (2002) Novel enzymatic method for the production of xylitol from D-arabitol by *Gluconobacter oxydans*. Biosci Biotechnol Biochem 66:2614–2620
4. Prust C, Hoffmeister M, Liesegang H, Wiezer A, Fricke WF, Ehrenreich A, Gottschalk G, Deppenmeier U (2005) Complete genome sequence of the acetic acid bacterium *Gluconobacter oxydans*. Nat Biotechnol 23:195–200
5. Liu D, Ke X, Hu Z-C, Zheng Y-G (2020) Combinational expression of D-sorbitol dehydrogenase and pyrroloquinoline quinone increases 6-(*N*-hydroxyethyl)-amino-6-deoxy-α-L-sorbofuranose production

by *Gluconobacter oxydans* through cofactor manipulation. Enzym Microb Technol 141:109670

6. Hu ZC, Bu JL, Wang RY, Ke X, Zheng YG (2019) Enhanced production of 6-(*N*-Hydroxyethyl)-amino-6-deoxy-α-L-sorbofuranose by immobilized *Gluconobacter oxydans* on corn stover with a pH control strategy in a bubble column bioreactor. Appl Biochem Biotechnol 188:297–309
7. Hu ZC, Zhao ZY, Ke X, Zheng YG (2020) Repeated production of 6-(*N*-hydroxyethyl)-amino-6-deoxy-α-L-sorbofuranose by immobilized *Gluconobacter oxydans* cells with a strategy of in-situ exhaustive cell regeneration. Bioprocess Biosyst Eng 43:1781–1789
8. Wang X, Liu J, Du G, Zhou J, Chen J (2013) Efficient production of L-sorbose from D-sorbitol by whole cell immobilization of *Gluconobacter oxydans* WSH-003. Biochem Eng J 77:171–176
9. Brenes RGR, Santos IMTS, de Carvalho LSC, Ramírez NIB, Pereira N Jr (2025) Characterization of 3D-printed acrylonitrile butadiene styrene and polylactic acid carrier-beads for *Gluconobacter oxydans* immobilization. J Biotechnol 406:154–167
10. Tang X, Hu W, Wang Z, Fan Y, Xu Y, Yong Q, Li X, Hua X (2025) Nanocellulose hydrogel-based living materials: enhancing microbial biotransformation of lignocellulosic biomass. Bioresour Technol, 133783
11. Abdelhamid MAA, Pack SP (2021) Biomimetic and bioinspired silicifications: Recent advances for biomaterial design and applications. Acta Biomater 120:38–56
12. Kong X, Chong X, Squire K, Wang AX (2018) Microfluidic diatomite analytical devices for illicit drug sensing with ppb-level sensitivity. Sens Actuators B 259:587–595
13. Kong X, Yu Q, Li E, Wang R, Liu Q, Wang AX (2018) Diatomite photonic crystals for facile on-chip chromatography and sensing of harmful ingredients from food. Materials 11:539
14. Ahmed A, Khan TA, Dan Ramdath D, Kendall CWC, Sievenpiper JL (2022) Rare sugars and their health effects in humans: a systematic review and narrative synthesis of the evidence from human trials. Nutr Rev 80:255–270
15. Bayramoglu G, Akbulut A, Arica MY (2013) Immobilization of tyrosinase on modified diatom biosilica: Enzymatic removal of phenolic compounds from aqueous solution. J Hazard Mater 244:528–536
16. Walsh PJ, Clarke SA, Julius M, Messersmith PB (2017) Exploratory testing of diatom silica to map the role of material attributes on cell fate. Sci Rep 7:14138
17. Abo-Shady AM, Zalat AA, Al-Ashkar EA, Ghobara MM (2019) Nanoporous silica of some Egyptian diatom frustules as a promising natural material. Nanosci Nanotechnology-Asia 9:414–425
18. Kim HJ, Kim JH, Shin CS (1999) Conversion of D-sorbitol to L-sorbose by Gluconobacter suboxydans cells co-immobilized with oxygen-carriers in alginate beads. Process Biochem 35:243–248
19. Fidaleo M, Charaniya S, Solheid C, Diel U, Laudon M, Ge H, Scriven LE, Flickinger MC (2006) A model system for increasing the intensity of whole-cell biocatalysis: Investigation of the rate of oxidation of D-sorbitol to L-sorbose by thin bi-layer latex coatings of non-growing *Gluconobacter oxydans*. Biotechnol Bioeng 95:446–458

20. Chacon SJ, Matias G, Ezeji TC, Maciel Filho R, Mariano AP (2021) Three-stage repeated-batch immobilized cell fermentation to produce butanol from non-detoxified sugarcane bagasse hemicellulose hydrolysates. Bioresour Technol 321:124504
21. Ocampo-López C, Ramírez-Carmona M, Rendón-Castrillón L, Muñoz-Blandón O, González-Pérez L, Ospina-Sanjuan Á (2023) Combined in-situ immobilization system of *Chlorella* sp. in photobioreactor. Case Stud Chem Environ Eng 8:100462
22. Santos DT, Sarrouh BF, Rivaldi JD, Converti A, Silva SS (2008) Use of sugarcane bagasse as biomaterial for cell immobilization for xylitol production. J Food Eng 86:542–548
23. Santos JC, Mussatto SI, Dragone G, Converti A, Silva SS (2005) Evaluation of porous glass and zeolite as cells carriers for xylitol production from sugarcane bagasse hydrolysate. Biochem Eng J 23:1–9

Figures

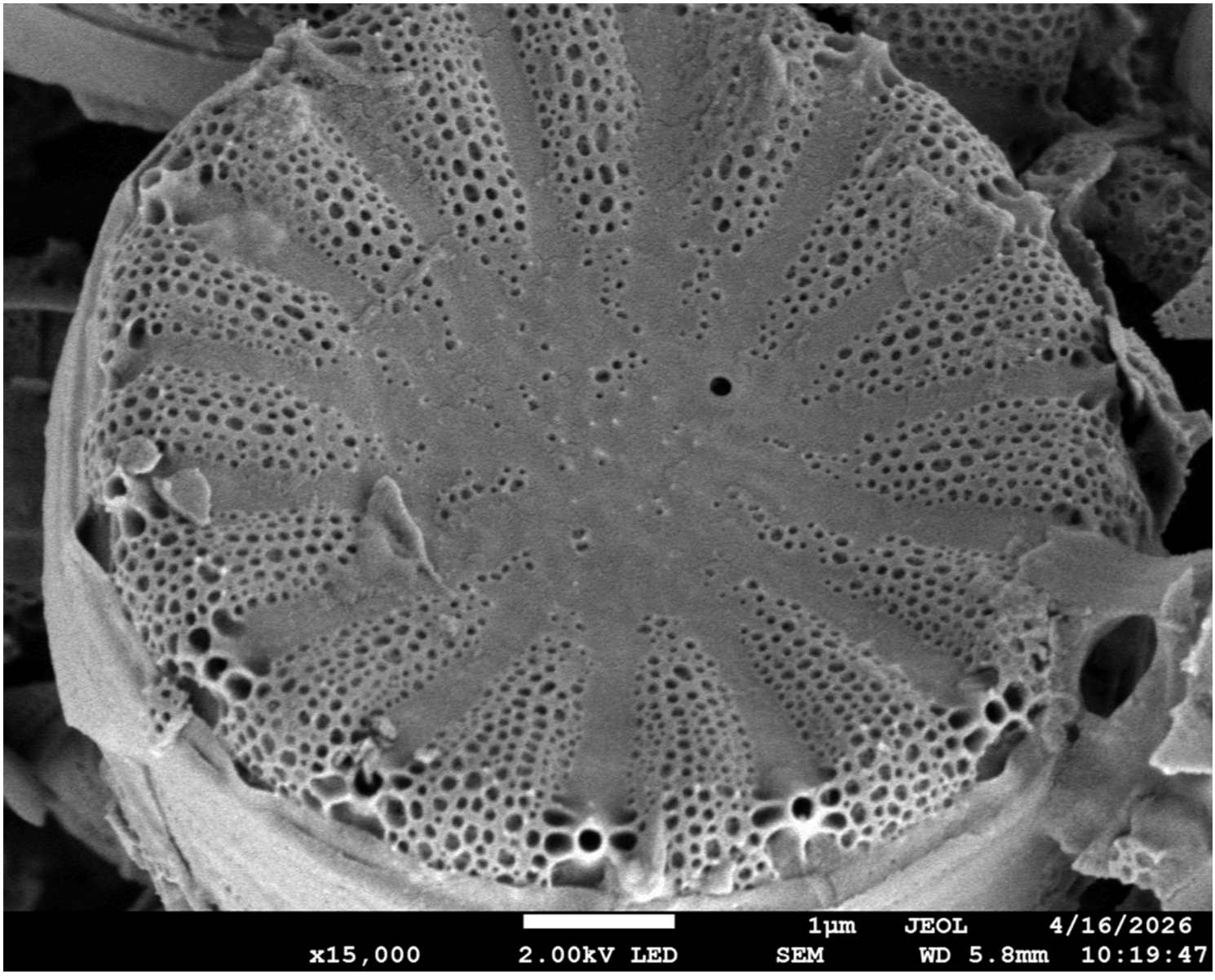


Figure 1

SEM micrographs of *C. meneghiniana* illustrate the different porosity scales

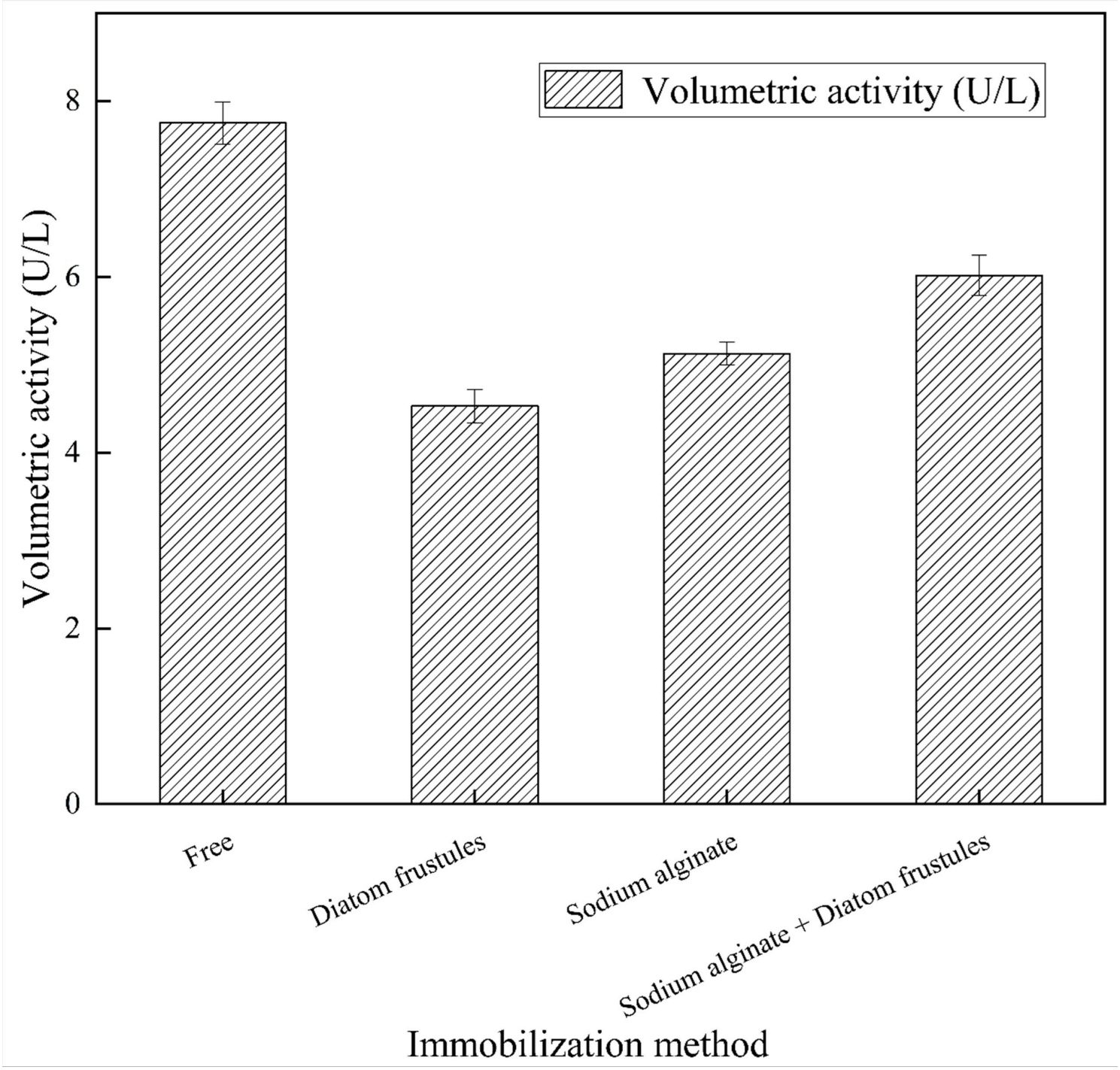


Figure 2

Enzymatic activity of recombinant *G. oxydans* immobilized on diverse carriers

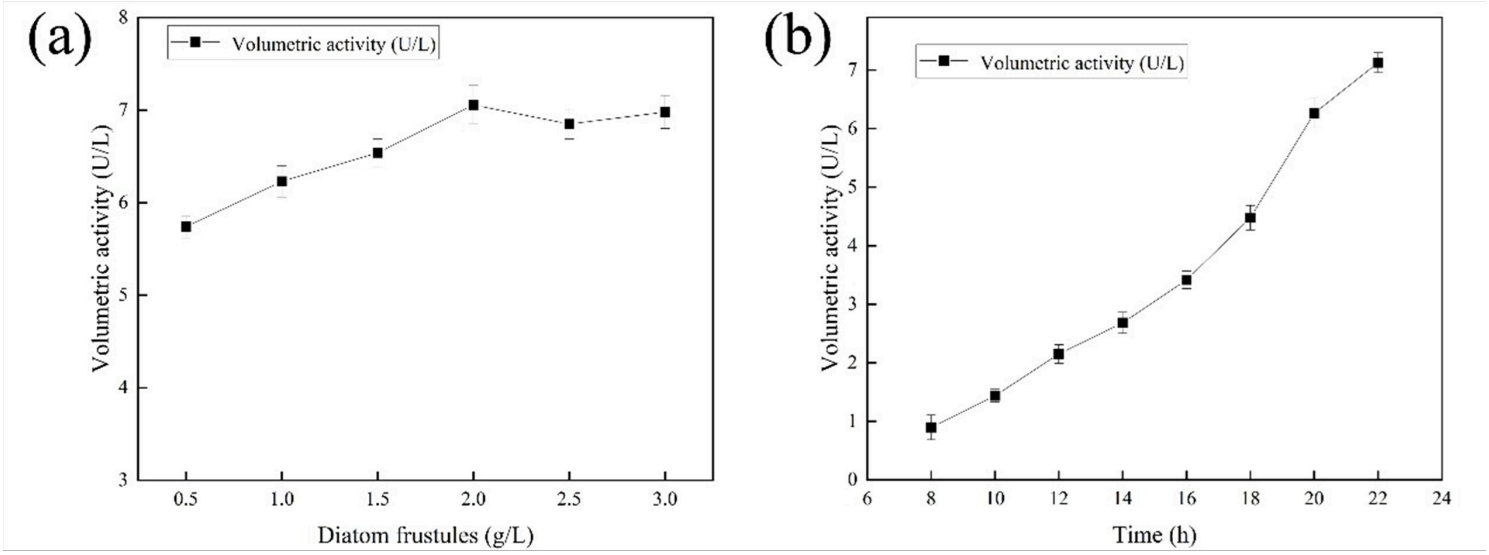


Figure 3

In-situ immobilization of recombinant *G. oxydans* on diatom frustules. (a) Effect of varying diatom frustule loading on the catalytic performance of immobilized *G. oxydans*. (b) Time course of *G. oxydans* adsorption onto diatom frustules

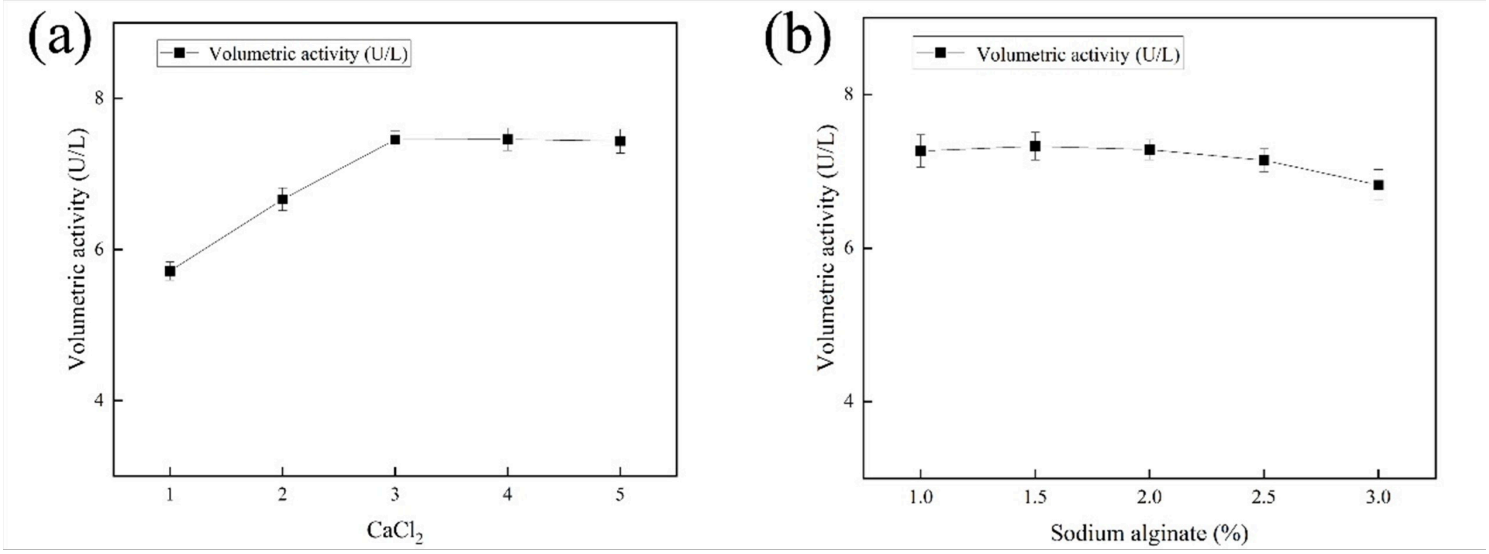


Figure 4

Effect of different $CaCl_2$ concentrations (a) and sodium alginate concentrations (b) on the catalytic performance of immobilized *G. oxydans*

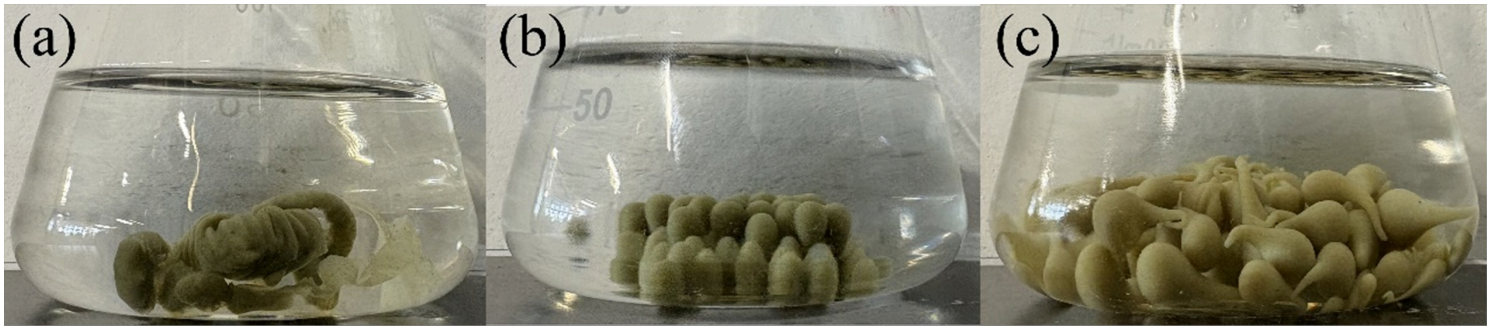


Figure 5

Effects of varying sodium alginate concentrations on bead morphology. (a) 1.0%; (b) 2.0%; (c) 2.5%

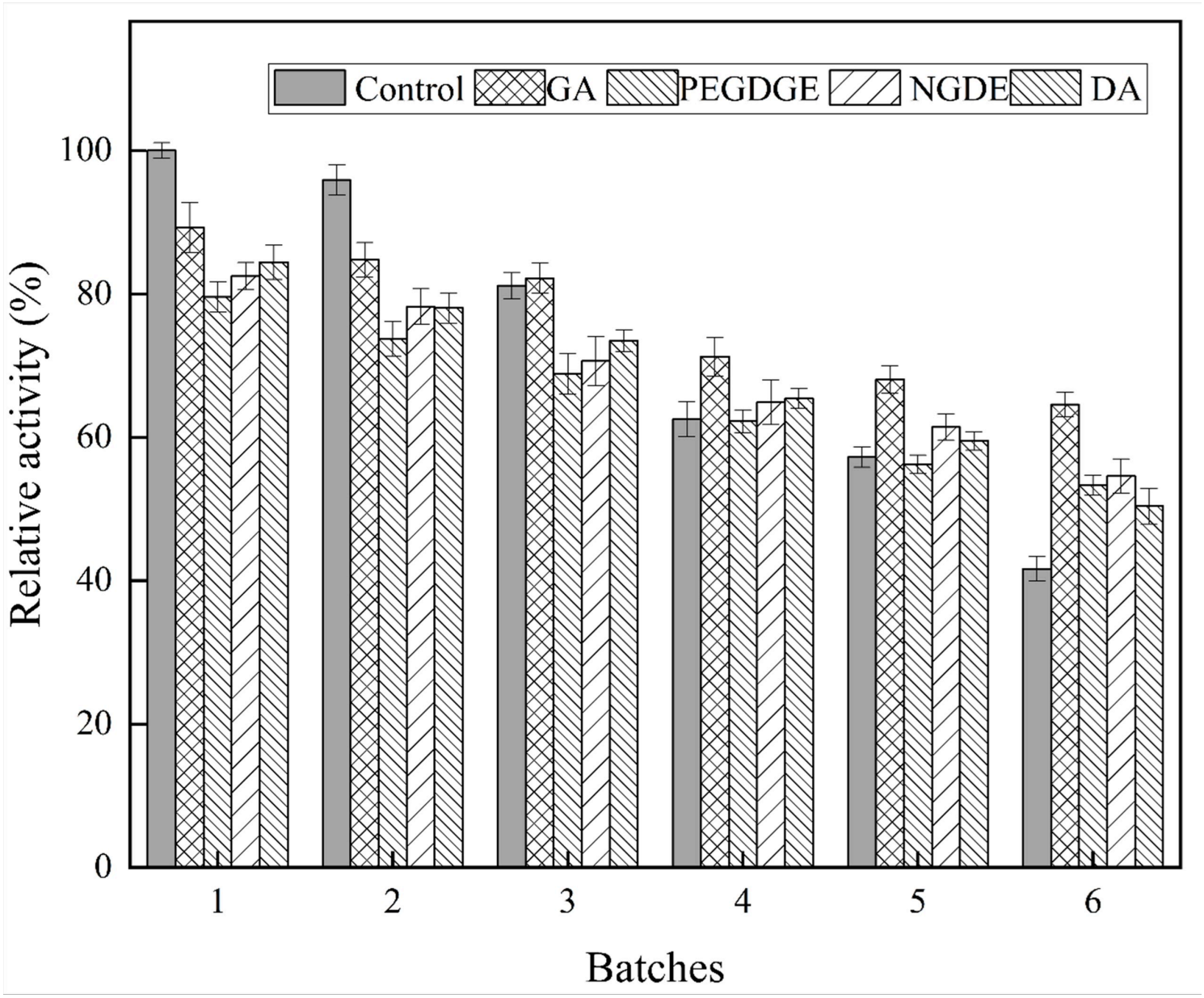


Figure 6

Effects of different crosslinking agents on the batch catalytic performance of immobilized *G. oxydans*

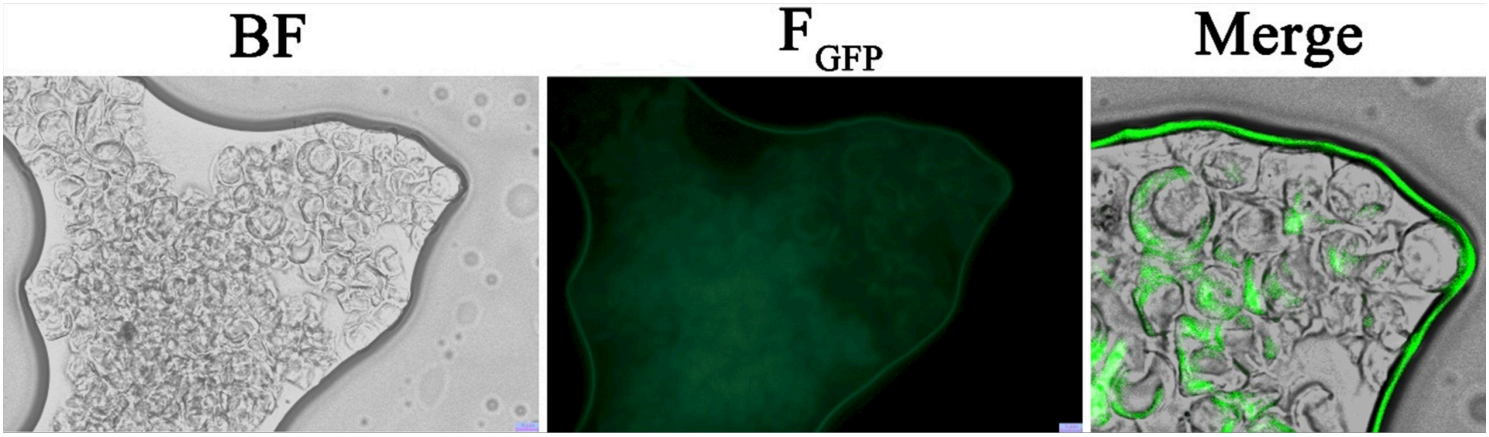


Figure 7

The GFP of diatom frustules with *G. oxydans*

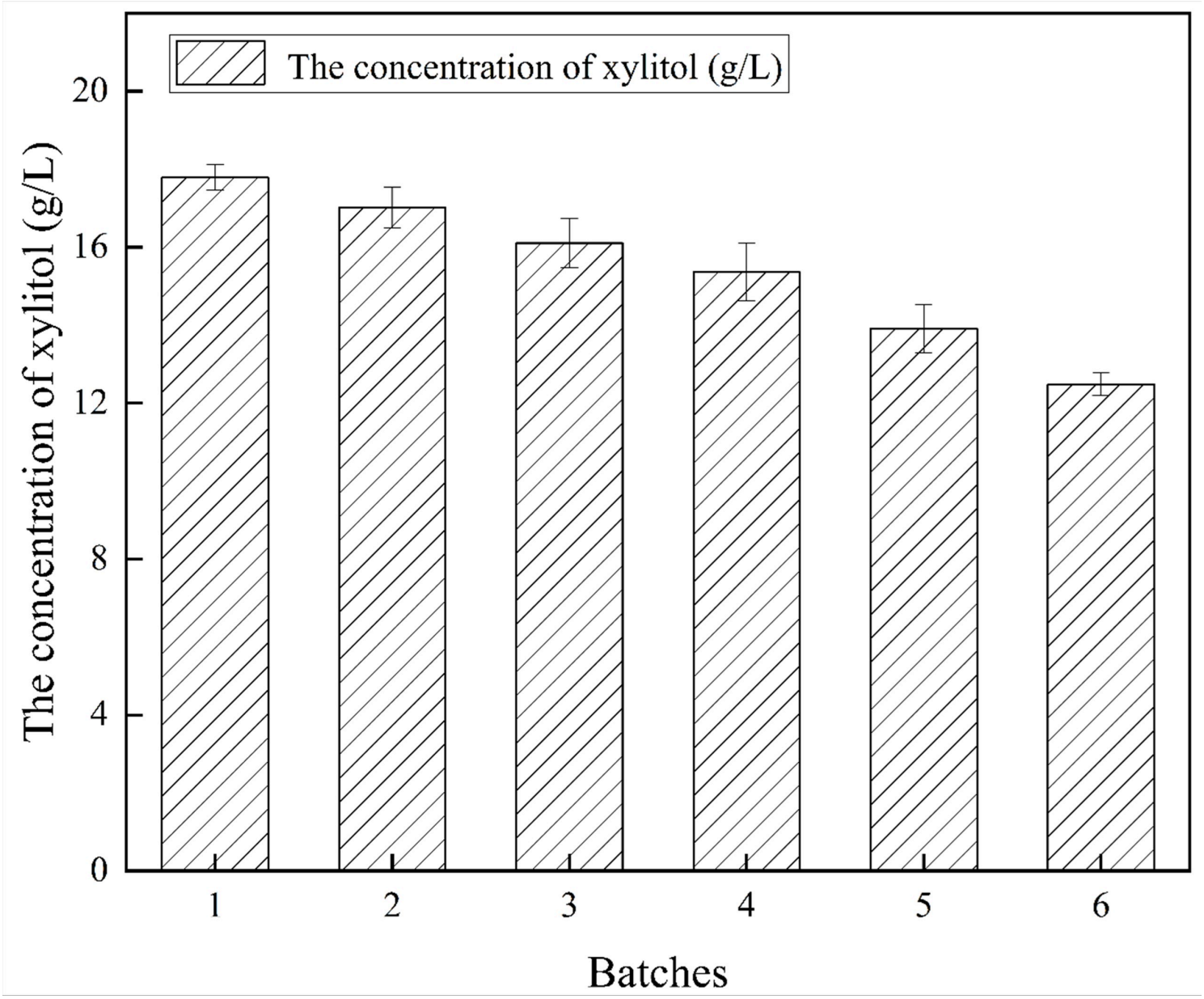


Figure 8

Reusability of immobilized *G. oxydans*